International Journal of Engineering Research and Science & Technology

www.ijerst.org

ISSN : 2319-5991

Vol. 21 No. 3 (1) 2025

ijerst.editor@gmail.com

editor@ijerst.com

International Journal of Engineering Research and Science & Technology

ISSN 2319-5991 www.ijerst.com
Vol. 21, No. 3(1), 2025

Research Paper

Enhanced Battery Longevity in EV Fast Charging with Based Active Damping in DAB converter

Jinka Keerthana[1], P.Thanuja[2]

[1]M. Tech Student, Department of Electrical and Electronics Engineering, Vaagdevi College of Engineering, Khammam - Warangal Hwy, Road, Bollikunta, Telangana 506005

[2]Associate Professor, Department of Electrical and Electronics Engineering, Vaagdevi College of Engineering, Khammam - Warangal Hwy, Road, Bollikunta, Telangana 506005

Abstract

The Dual Active Bridge (DAB) converter is well adapted for DC micro grid- connected EVCS applications as well as off-board rapid EVCS. However, since the charging current is quite strong and any oscillations would impair the EV battery life, careful adjustment of the DAB converter architecture is essential for rapid charging. According to published research, EV battery charging using a DAB converter architecture combined with a series inductor at the output lowers output current ripple by 40%.

However, we have found that adding an LC filter to the system introduces potentially unstable dynamics. Since this impacts the stability of the controller, active or passive damping is required to reduce these dynamics. The significant losses that passive damping generates, which are partially caused by switching-frequency noise and partially by low-frequency noise, make it less effective. It is also quite difficult to place the dampening at the selected resonant frequency. The most used control algorithm in industry is proportional integral derivative (PID) control, which is well recognized in the field of industrial control. PID controllers' wide spread use may be ascribed in part to their reliable operation under a variety of operating situations and in part to their as of use, which enables engineers to run them withease. In this current study in addition to the existing system we are using PID controller as extension for checking the simulation results.

Received: 11-07-2025 Accepted: 25-07-2025 Published: 13-08-2025

1. Introduction

With the recent evolutions in battery technology and the growing number of Electric Vehicles (EV), the development of a fast EV charging station (EVCS) is necessary. Fast charging is a significant concern for the power grid as it demands high current in a very short span. As its impact is more pronounced during peak hours, efficient load-side management techniques are required. One possible solution is to incorporate EV and EVCS as a part of the local microgrid for vehicle-to-grid (V2G) and gridto-vehicle (G2V) energy exchange [1], [2]. Due to their mobility and energy storage capabilities, EVs can be an ideal energy source for the microgrid system. A microgrid setup lowers transmission losses and improves grid reliability [3]. A DC microgrid features higher efficiency, faster dynamic response, and improved current carrying capability than an AC microgrid [4], [5]. In addition, it adds more natural connect to several renewable energy sources (RESs), energy storage devices (ESDs) and EV loads [6]. All these factors result in the enhanced DC microgrid-type power structure for remotely located homes, military services, data and telecommunication hubs, EVCSs, ships, etc. [7]. Researchers are focusing on bidirectional battery power flow due to the advancements in battery technology that has enhanced life, cycle times, charging rates (C-rates), and power density [8], [9]. For DC microgrids, dc/dc converters with modular structure, isolation and bidirectional capabilities are crucial. These converters must aid with power flow back to the grid during peak hours and charge the battery when operating in the forward mode. DC level-3 and rapid EVCS delivering high current to EV can be interfaced to a DC microgrid using a dc/dc converter without any additional AC/DC converter. Multiple dc/dc converters can be stacked together within an

EVCS to boost the output power for fast charging. These stacked converters can also act as solid-state transformers (SSTs) to regulate power exchange between the load and the microgrid [10]. In literature, different types of isolated bidirectional dc/dc converter (IBDC) topologies have been reported, which include three-phase push-pull [11], dual flyback [12], bidirectional-LLC resonant converter [13], dual-Cuk [14], and dual active bridge (DAB) [15]. DAB is one of the promising IBDC topologies for microgrids, energy storage applications, and EVCS due to soft-switching commutation, low device count, and high efficiency [16]- [18]. The design is ideal for applications where cost, power density, isolation, reliability, weight, and high voltage conversion factor are crucial. DAB's modularity and symmetrical configuration enable stacking converters for high power throughput and allow bidirectional operation. Mukherjee et al. demonstrates that the DAB converter outperforms the LLC and other converters when operated under heavy load, resulting in 27% loss reduction compared to LLC converter. Numerous DAB applications have been reported in the literature. Power grids have implemented SSTs built with DAB to connect different-scale microgrids at different dc voltage levels. The DAB-based high-frequency power transformer for traction applications is very effective. It offers new features like HV insulation and low heat dissipation and is lighter than the traditional onboard line frequency transformers. DAB has become a practical choice for onboard battery chargers for plug-in EVs. Other applications include uninterrupted power supplies (UPS), ESD interface converters, power-load emulators, and airborne wind turbines. Modeling the DAB converter and designing a controller with specific steady-state and dynamic performance is crucial for all these applications. Current research on DAB converters in EV charging includes improved strategies for zero voltage switching (ZVS), elimination of circulating current flow [29], improvement in current carrying capacity for fast EVCS, high-frequency transformer saturation prevention, electrical design optimization, and cost-effective controller design. Costa et al. have modeled the DAB converter for EV charging by considering an inductor in series with the battery to reduce current ripples. Iyer et al. have addressed the DC-link stability issues that emerge during DAB interfacing by using a virtual-resistance scheme. To improve DAB functionality, wide-ranging research on converter structural enhancements is also in progress. In , a modular DAB topology is proposed by splitting one of the bridge legs and transformer, to increase control freedom for wide voltage variations in plug-in EV charging loads. Study in suggests using ring-connected DAB in a multiport DC-DC converter for fast EVCS to increase power availability. A modified series-parallel resonant three-level DAB converter with ZVS operation, giving good performance in constant current constant voltage (CCCV) charging mode and short-circuited situations, is proposed in.

A modified DAB-converter topology with a high transformation ratio scheme is implemented in, to optimize conversion efficiency. Several optimization techniques are employed in DAB control with the objective of optimizing efficiency, ZVS operation, and inductor rms-current stress. Chaurasiya et al. uses particle-swarm-optimization to minimize voltage and current stress for a wide voltage off-board fast EV charger using three-level DAB. Gong et al. proposed a multi objective optimization-based modulation strategy to extend the ZVS range and achieve quasi-optimal inductor rms current stress over the entire working range of EV chargers. In, a modified DAB-based charging module for fast EVCS with minimum rms current stress is proposed, wherein optimized converter parameters are obtained using genetic algorithm. Study in used a multiple-duty modulation scheme to improve charging efficiency, achieve ZVS and minimize rms current stress. Haque et al. proposed DAB with ZVS and reactive power (Q) control capability for an EV using mixed-modulation approach and a Q-optimization algorithm using load flow concepts. In, optimal duty modulation using Lagrange-multipler is proposed to realize ZVS and reduce peak-to-peak and rms current stress. In this paper, a DAB converter and its controller are designed for EVCS, which will be connected to a DC microgrid for fast charging applications.

The proposed scheme reduces the error at the resonant frequency, thereby decreasing the output voltage and current ripple and improves the dynamic performance of the entire EV charging system. It also avoids the requirement of additional sensors for measuring filter current and voltage by selective attenuation of the desired frequency. The battery is discharged by reversing the phase shift between

bridges in constant current (CC) mode. CCCV algorithm is used for battery charging. The major contributions of the paper are as follows:-

1) Design of DAB converter along with the topological modifications for reduced battery degradation during fast charging.

2) Proposed a novel and robust active damping approach using a twin-T NF to damp the potentially unstable dynamics.

2. Electric vehicle

Electric Vehicle (EV) is an emerging technology in the modern world because of the fact that it mitigates environmental pollutions and at the same time increases fuel efficiency of the vehicles. Multilevel inverter controls electric drive of EV of high power and enhances its performance which is the reflection of the fact that it can generate sinusoidal voltages with only fundamental switching frequency and have almost no electromagnetic interference. This paper describes precisely various topology of EVs and presents transformer less multilevel converter for high voltage and high current EV. The cascaded inverter is IGBT based and it is fired in a sequence. It is natural fit for EV as it uses separate level of dc sources which are in form of batteries or fuel cells. Compared to conventional vehicles, hybrid electric vehicles (EVs) are more fuel efficient due to the optimization of the engine operation and recovery of kinetic energy during braking. With the plug-in option (PEV), the vehicle can be operated on electric-only modes for a driving range of up to 30–60 km. The HEVs are charged overnight from the electric power grid where energy can be generated from renewable sources such as wind and solar energy and from nuclear energy. Fuel cell vehicles (FCV) use hydrogen as fuel to produce electricity, therefore they are basically emission free. When connected to electric power grid (V2G), the FCV can provide electricity for emergency power backup during a power outage. Due to hydrogen production, storage, and the technical limitations of fuel cells at the present time, FCVs are not available to the general public yet. EVs are likely to dominate the advanced propulsion in coming years. Hybrid technologies can be used for almost all kinds of fuels and engines. Therefore, it is not a transition technology. In EVs and FCVs, there are more electrical components used, such as electric machines, power electronic converters, batteries, ultra capacitors, sensors, and microcontrollers. In addition to these electrification components or subsystems, conventional internal combustion engines (ICE), and mechanical and hydraulic systems may still be present. The challenge presented by these advanced propulsion systems include advanced powertrain components design, such as power electronic converters, electric machines and energy storage; power management; modeling and simulation of the powertrain system; hybrid control theory and optimization of vehicle control

In recent years, research in electric vehicle (EV) development has been focused on various aspect of design, such as component architecture, engine efficiency, reduced fuel emissions, material for lighter components, power electronics, efficient motors and high power density batteries. To meet some of the aspect of EV cascaded multilevel inverter is used so as to meet high power demands. The multilevel voltage source inverters with unique structure allow them to reach high voltages with low harmonics without the use of transformers or series-connected synchronized switching devices. The general function of the multilevel inverter is to synthesize a desired voltage from several levels of dc voltages. For this reason, multilevel inverters can easily provide the high power required of a large electric drive. As the number of levels increases, the synthesized output waveform has more steps, which produces a staircase wave that approaches a desired waveform. Also, as more steps are added to the waveform, the harmonic distortion of the output wave decreases, approaching zero as the number of levels increases. As the number of levels increases, the voltage that can be spanned by summing multiple voltage levels also increases.

The structure of the multilevel inverter is such that no voltage sharing problems are encountered by the active devices. HEV Configurations

2.2 Why EV'S, HV'S?

HEV Configurations

Vehicles equipped with conventional internal combustion engines (ICE) have been in existence for over 100 years. With the increase of the world population, the demand for vehicles for personal transportation has increased dramatically in the past decade. This trend of increase will only intensify with the catching up of developing countries, such as China, India, and Mexico. The demand for oil has increased significantly. Another problem associated with the ever-increasing use of personal vehicles is the emissions. The greenhouse effect, also known as global warming, is a serious issue that we have to face. There have been increased tensions in part of the world due to the energy crisis. Government agencies and organizations have developed more stringent standards for the fuel consumption and emissions. Nevertheless, with the ICE technology being matured over the past 100 years, although it will continue to improve with the aid of automotive electronic technology, it will mainly rely on alternative evolution approaches to significantly improve the fuel economy and reduce emissions. Battery-powered electric vehicles were one of the solutions proposed to tackle the energy crisis and global warming. However, the high initial cost, short driving range, long charging (refueling) time, and reduced passenger and cargo space have proved the limitation of battery-powered EVs. The HEV was developed to overcome the disadvantages of both ICE vehicles and the pure battery-powered electric vehicle. The HEV uses the onboard ICE to convert energy from the onboard gasoline or diesel to mechanical energy, which is used to drive the onboard electric motor, in the case of a series HEV, or to drive the wheels together with an electric motor, in the case of parallel or complex HEV. The onboard electric motor(s) serves as a device to optimize the efficiency of the ICE, as well as recover the kinetic energy during braking or coasting of the vehicle. The ICE can be stopped if the vehicle is at a stop, or if vehicle speed is lower than a preset threshold, and the electric motor is used to drive the vehicle along. The ICE operation is optimized by adjusting the speed and torque of the engine. The electric motor uses the excess power of the engine to charge battery if the engine generates more power than the driver demands or to provide additional power to assist the driving if the engine cannot provide the power required by the driver. Due to the optimized operation of the ICE, the maintenance of the vehicle can be significantly reduced, such as oil changes, exhaust repairs, and brake replacement. In addition, the onboard electric motor provides more flexibility and controllability to the vehicle control, such as antilock braking (ABS) and vehicle stability control (VSC).

3. Modeling of case study

3.1 Existing dab topology

In the DAB converter, shown in Fig. 5.1(a), power is transferred by turning ON the MOSFET switches, which generates phase-shifted high-frequency square waves on the primary and secondary sides of the transformer. The power flows from the leading bridge to the lagging bridge, as shown in Fig. 5.1(b). The direction of the power flow can be reversed by reversing the phase shift. Moreover, the turning ON/OFF of the diagonal switches happen simultaneously, resulting in a square wave at the output of each bridge. The duty ratio of the primary and secondary bridge switches is set to 50%.The most critical factor in designing the power stage of DAB include the choice of coupling inductor, switching frequency, phase shift, design of transformer magnetics, and desired ZVS range.

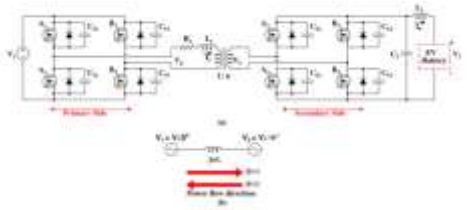

FIGURE 1 (a) DAB converter conventional topology (b) Operating principle.

Most of these design factors are interdependent. For instance, the phase shift of the converter's operation

at the target power level depends directly on the maximum power transfer, which in turn depends on the coupling inductor selection. Switching frequency (fs) decides the efficiency and power density of the converter. Using SiC MOSFETs in the power stage allows the converter to operate at high fs . Higher fs makes it possible to use smaller magnetics, which improves the thermal solution and raises the converter's power density. Therefore, the allowable heat sink solution and transformer size are traded off when selecting fs for a specific target efficiency. Moreover, if the chosen MOSFET has high output capacitance, setting high fs results in significant switching losses at light loads, thereby reducing the efficiency. Thus, the selection of fs significantly impacts the implementation of the control loop bandwidth. The auxiliary inductor (L1) manages the power transfer, which directly adds to the transformer inductance in DAB. The LC filter connected across the battery terminal minimizes the ripples in the charging/discharging current.

3.2 Proposed dab topology

We analysed that the LC filter connected across the DAB converter output for lowering the ripple content induces unstable dynamics in the system. These unstable dynamics occurring at the switching frequency and LC filter resonant frequency can significantly result in large voltage ripples at the output, which can cause problems in sensitive loads and reduce system efficiency. Overshoot can lead to instability in the control loop, causing excessive oscillations and reduction of the system's overall stability. It can trigger the over-current protection, causing the converter to shut down or reduce its output power, leading to power interruptions or reductions. The overshoot can cause the battery voltage to go above the rated maximum voltage, which can cause permanent damage and reduce its lifespan. Additionally, it can result in a high current surge in the battery, causing thermal stress on the cells, overheating, and further damage. Also, it may cause excessive battery discharge, which can reduce the battery's available capacity. In addition, overshoot can also lead to poor regulation of the battery voltage, which can cause instabilities in the system and affect the performance of the EV. Hence, minimising overshoot in the DAB converter is crucial to avoid damage to the battery and guarantee optimal system performance.

3.3 Proposed dab topology

The frequency at which the system exhibits unstable dynamics is found to be equal to the resonant frequency of the output LC filter, given by fr = 1/(2π √ L2C2). Substituting for L2 and C2, gives fr equal to 46625 rad/sec. These oscillations can be damped using either active or passive damping. Compared to passive, active damping offers a selective placement and loss reduction. Passive damping is less efficient due to its considerable losses, partly induced by low-frequency noise and partly from switching frequency noise. The passive damping solution is less effective as placing the damping at the selective resonant frequency is very complex. Active damping, on the other hand, involves modification of the structure of the controller or changing the control parameters to achieve desired gain margin (GM) and phase margin (PM) around the appropriate resonant frequency. Moreover, to carry out active damping, the sampling rate or the control frequency must be two times the resonance frequency to control the unstable dynamics effectively. In this paper, we have proposed a robust and straightforward method for EV battery charging using a DAB converter that uses active damping to eliminate unstable dynamics. Here, the existing DAB topology is modified by cascading a twin-T notch filter, with parameters R = 214 Ω and C = 0.1 µF at the output, as shown in Fig. 5.2 The designed filter can be connected directly across the converter. The effective impedance Z0 of the cascade connection of battery and filter is given by (30), as shown at the bottom of the next page.

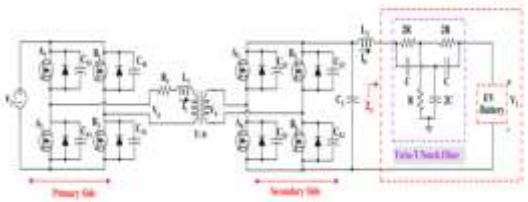

FIGURE.2 Proposed DAB converter topology considering twin-T notch filter in cascade.

$$Z_0 = \frac{16.24 \times 10^{25} s^3 + 29.52 \times 10^{34} s^2 + 27.52 \times 10^{39} s + 6.4 \times 10^{44}}{1.48 \times 10^{28} s^3 + 3.44 \times 10^{37} s^2 + 1.6 \times 10^{56} s + 1.5 \times 10^{42}} \quad (1)$$

International Journal of Engineering Research and Science & Technology

$$G_{ol,p} = \frac{6\times10^{9}s^{4}+10^{12}s^{3}+3\times10^{15}s^{2}+3\times10^{25}s+6\times10^{27}}{s^{5}+2\times10^{3}s^{4}+5\times10^{11}s^{3}+4.6\times10^{15}s^{2}+10^{21}s+2.5\times10^{23}} \quad (2)$$

$$G^{cl}_{v} = \frac{s_{4}+3\times10_{8}s_{3}+2\times10_{11}s_{2}+s\times10_{16}s_{2}+10_{23}s+3\cdot2\times10_{22}}{10_{11}s_{3}+3\times10_{16}s_{2}+1\cdot2\times10_{21}s+1\cdot s\times10_{23}} \quad (3)$$

The GM and PM are obtained for the open-loop system to determine system stability. GM very close to unity and PM nearing zero implies the system has oscillatory behaviour, while large GM or PM indicates a sluggish response. A balance between both is usually set up to obtain good relative stability. However, as the battery load is dynamic and any overshoot will result in the degradation of the battery, slow response time and high PM are selected. Accordingly, after choosing the performance parameters, the PID controller is tuned so that the error between the desired and actual parameters approaches zero. The gain cross-over frequency (ωgc) sets the control bandwidth. High ωgc increases the response time at the cost of reduced stability. Considering this, we have chosen PM=90◦ and ωgc is set to 7 rad/sec and 0.2 rad/sec for the current and voltage controller, respectively. The modified PID controller structure is shown in Fig.5.3, and the performance parameters are specified in Table 3. Theoretically, the system's stability can be improved by reducing the proportional gain of the PID controller, but at the cost of reduced bandwidth [48].

TABLE 1 PID controller parameters with active damping.

Controller Type	Parameter
Current Control	$K_P = 5.28\times10^{-4}$
	$K_I = 0.124$
Voltage Control	$K_I = 8.28\times10^{-6}$

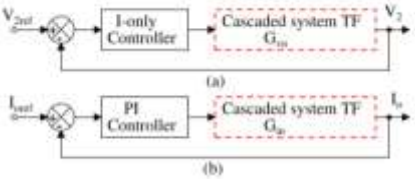

FIGURE 3 Controller design for the cascaded system in (a) Voltage control mode (b) Current control mode

The proposed active damping method not only achieves resonance damping but also improves the proportional gain of the PID controller, thus satisfying the requirement of bandwidth. Moreover, the proposed method also aids in the improvement of the robustness margin by handling parameter uncertainties and improving the system stability. The proposed scheme for design and implementation of filter-based active damping of the DAB converter for EV fast charging is demonstrated in Algorithm 1.

Algorithm 1 Scheme for Design and Active Damping of the DAB Converter for EV Fast Charging

1) Read input voltage (V1), output voltage (V2), EV battery rated capacity (Ah) and nominal voltage (VBatt).

2) For the designed DAB converter V1 = 600 V, V2 = 380 V and VBatt = 320 V. The values are chosen to facilitate EVCS connection to a 600 V DC microgrid.

3) Compute the value of coupling inductor L1 using (21).

4) Compute phase shif

$$\phi = \frac{\pi}{2}\left(1-\sqrt{1-\frac{8f_sL_1P_0}{nV_1V_2}}\right)$$

5) Compute output capacitor (C2) and output inductor (L2) using,

$$C_2\frac{dV_2}{dt} = \frac{V_1}{2\pi f_s nL_1}\frac{\phi}{\pi}\left(1-\frac{\phi}{\pi}\right) - \frac{V_2}{R_0} \quad \text{and}$$

$$L_2\frac{di_0}{dt} = \frac{V_1}{2\pi f_s nL_1}\frac{\phi}{\pi}\left(1-\frac{\phi}{\pi}\right)\frac{1}{\omega_s C_2} - I_0\left(R_0+\frac{1}{\omega_s C_2}\right).$$

6) Compute the resonance frequency of the output LC filter, fr = 1/(2π √ L2C2)

7) Compute R for the twin-T notch filter using R = 1/(2πCfr) considering C = 0.1 µF.

8) Compute the effective impedance Z0 using nodal analysis as given in (30).

9) Compute the TF (for CV mode)

$$\frac{V_2(s)}{\phi(s)} = \frac{V_1}{2n\pi L_1 f_s}\left(1-\frac{2\phi}{\pi}\right)\frac{sL_2+Z_0}{s^2C_2L_2+sC_2Z_0+1}$$

10) Compute the TF (for CC mode):

$$\frac{i_0(s)}{\phi(s)} = \frac{V_1}{2n\pi L_1 f_s}\left(1-\frac{2\phi}{\pi}\right)\frac{1}{s^2C_2L_2+sC_2Z_0+1}$$

11) Compute the controller parameters by setting appropriate PM and ωgc.

The proposed system is used for charging the Li-ion battery. Li-ion is preferred in most EVs owing to the high energy density requirement during driving. We have used CCCV algorithm [49] for the battery charging. In CCCV at low SoC, battery charging occurs in the constant current mode, wherein the charging process begins with a constant current value. This value is set based on the desired C-rate andthis mode lasts until the battery voltage attains an equalization value (Veq). After that, charging enters constant voltage mode. The voltage is kept constant, and the charging current reduces naturally. The flowchart for the battery charging and discharging control is shown in Fig. 4

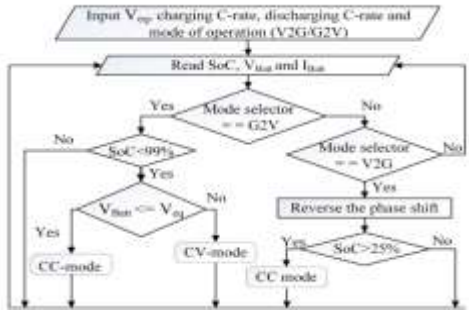

FIGURE 4 Flowchart for the battery charging and discharging control

3.4 PID Controller

A PID controller is an instrument used to maintain a process variable, such as temperature, flow, pressure, or speed, at a desired set point. These devices continuously measure the difference between the set point and the actual value, adjusting output to minimize that difference. Because they adapt so easily to different processes, these devices are integral to operations across many industries. They can seamlessly switch between maintaining tight temperature control in a pharmaceutical reactor, regulating air flow in an HVAC system, or adjusting feed rates in a packaging line all while minimizing fluctuations and ensuring product quality.

A PID controller constantly measures process variables and compares them to the desired set point. It then calculates how much correction is needed and adjusts to bring the process back on target. What makes a PID controller especially powerful is how it combines three control strategies into one seamless response:

SIMULATION RESULTS

Proposed model and results

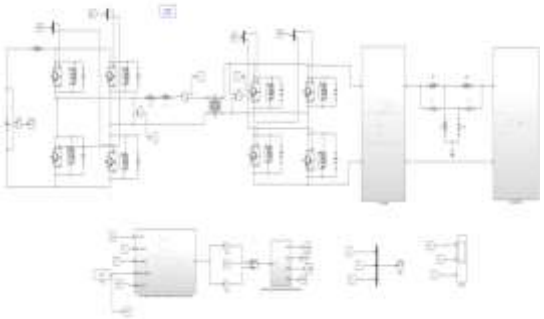

FIGURE 5.1 Simulink Model of the proposed DAB converter topology considering twin-T notch filter in cascade.

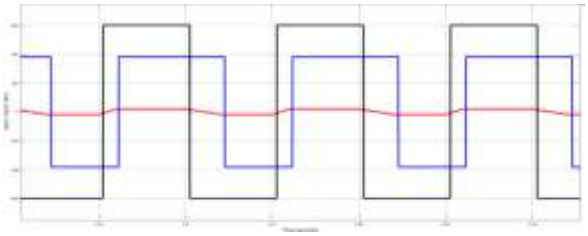

FIGURE 5.2 Primary and secondary side bridge voltages and inductor current.

The MATLAB Simulink block diagram of the proposed model is shown in Fig. 5.1 The simulation of closed-loop operation is initially carried out by considering a nominal resistive (R) load of 14.44Ohms using current control and voltage control modes separately. The primary (Vp) and secondary (Vs) bridge voltages and the coupling inductor current (I1) waveform is shown in Fig. 5.2

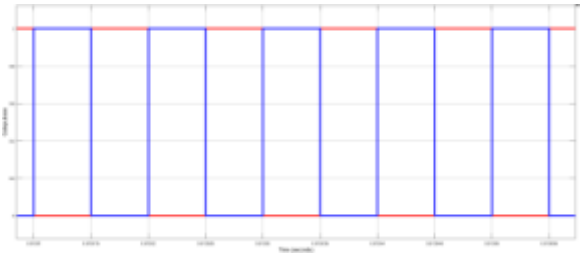

FIGURE 5.3 Zero Voltage Switching (ZVS) for MOSFET switches

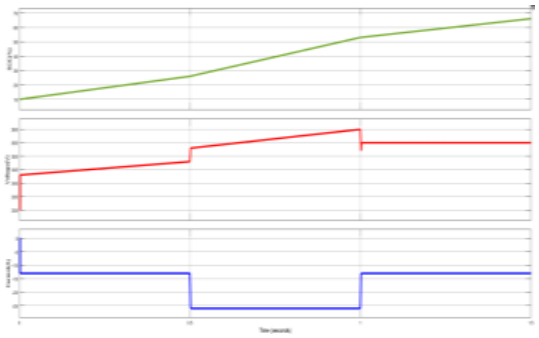

FIGURE 5.4 Battery parameter variation viz. SoC, voltage (V2) and current (I0) while charging at 1C-rate and 2C-rate.

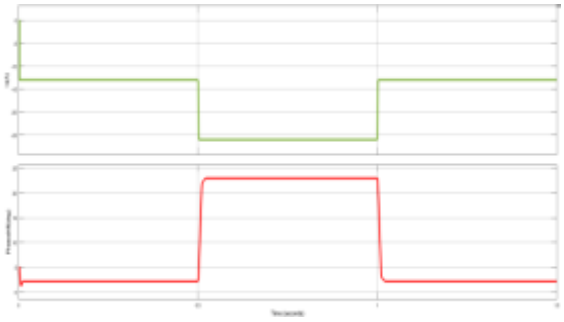

FIGURE 5.5 Variation in phase-shift with change in C-rate.

The ZVS of primary and secondary bridge switches is shown in Fig. 5.3. Subsequently, a battery load is connected. For demonstration, we have chosen a battery with a nominal voltage (VBatt) of 320 V and a capacity of 13 Ah, for which Veq is 372.47 V. The battery is charged at 2C rate to indicate fast charging, and the charge is controlled using the CCCV algorithm. Battery parameter variation viz.

SoC, voltage (V2) and current (I0) while charging in a closed-loop mode for varying C-rates isshown in Fig. 5.4 It is observed that the SoC of the battery is gradually increasing from 10% to 66% in response to the change in C-rate. For the performance evaluation of the developed CCCV controller, the C-rate of the battery was varied from 1C to 2C and again was brought back to 1C by step changing the current drawl (negative direction) from 13 A to 26 A and then reducing back to 13 A as indicated in Fig. 5.5

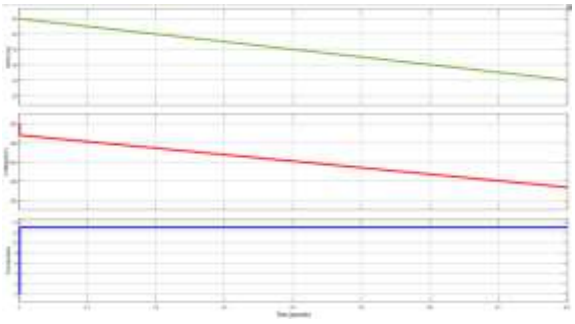

FIGURE 5.6 Battery parameter variation viz. SoC, voltage (V2) and dc-link current (Is) while discharging the battery at 1C-rate.

It is observed that the phase shift is accordingly increased from2.16◦ to 23◦ and then rolled back to 2.16◦ , thus validating the robustness of the designed controller and theoretical phase-shift computation. Reversing the phase shift between the primary and secondary bridges results in the power flow from the vehicle to the grid.

The battery was discharged at 1C rate under CC mode to verify bidirectional operation. The waveform in Fig. 5.6 depicts a drop in battery SoC from 50% to 25% along with a corresponding decrease in the battery voltage, while keeping current in the dc link, Is at the constant magnitude. To preserve the longevity, performance, and safety of the battery, the SoC is not permitted to drop below 25% while discharging to the grid

Extension model and results with PID

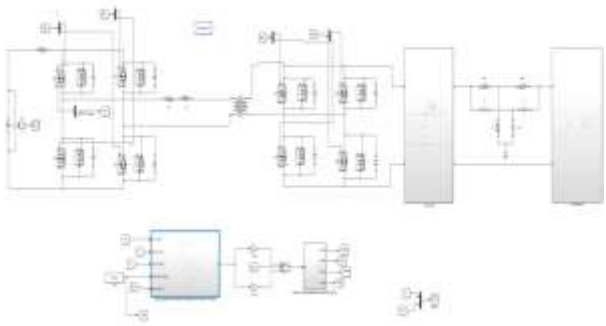

FIGURE 5.7 Simulink Model of the proposed DAB converter topology considering twin-T notch filter in cascade by using PID controller

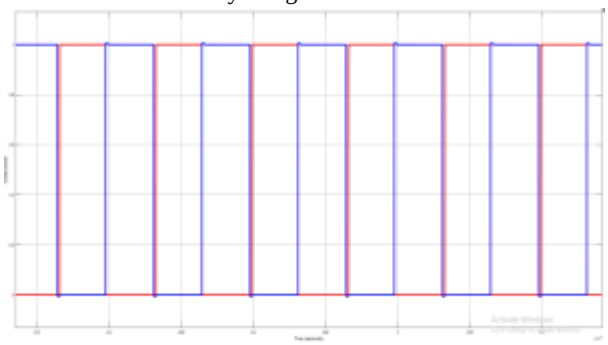

FIGURE 5.8 Zero Voltage Switching (ZVS) for MOSFET switches

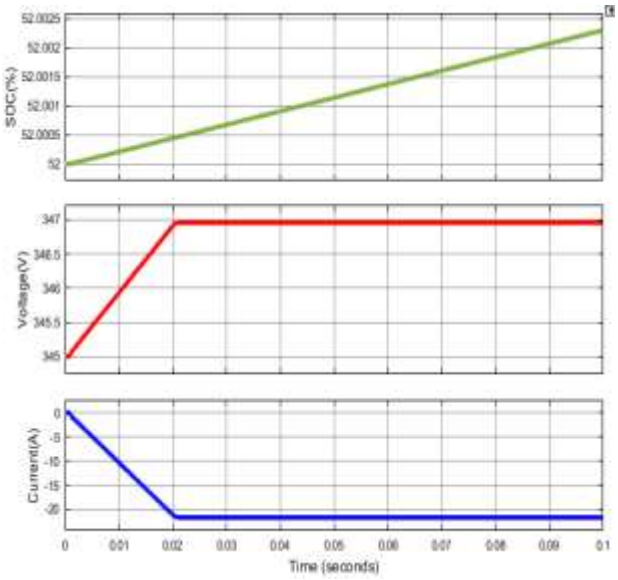

FIGURE 5.9 Battery parameter variation viz. SoC, voltage (V2) and current (I0) while charging at 1C-rate and 2C-rate

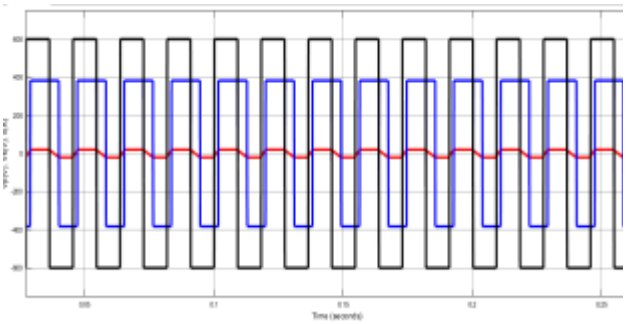

FIGURE 5.10 Primary and secondary side bridge voltages and inductor current

Figure 5.8 shows the zero-voltage-switching (ZVS) of main and secondary bridge switches that use PID. After that, a load for the battery is attached. A 13 Ah battery with a nominal voltage (VBatt) of 320 V and a Veq of 372.47 V will be used for the experiment. The CCCV algorithm controls the charging of the battery, which is done at a 2C pace to signify quick charging.

Fig. 5.9 shows the fluctuation of battery parameters, including state of charge (SoC), voltage (V2), and current (I0), while charging in a closed-loop mode using a PID controller for different C-rates. It has been noted that when the C-rate changes, the battery's SoC increases, going from 10% to 66%. Figure 5.10 shows the steps used to evaluate the performance of the CCCV controller that was built. First, the battery's C-rate was altered from 1C to 2C. Then, the current drawl was reduced from 26 A to 13 A, and finally, it was increased back to 1C.

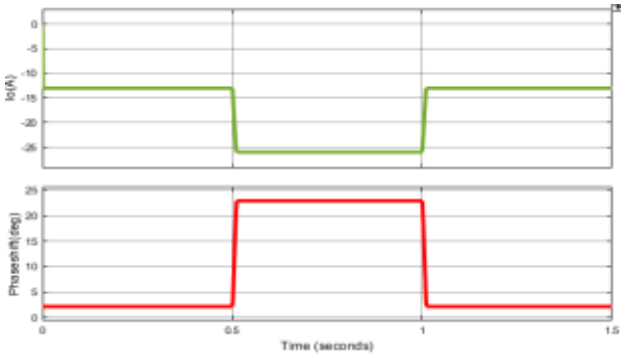

FIGURE 5.11 Variation in phase-shift with change in C-rate

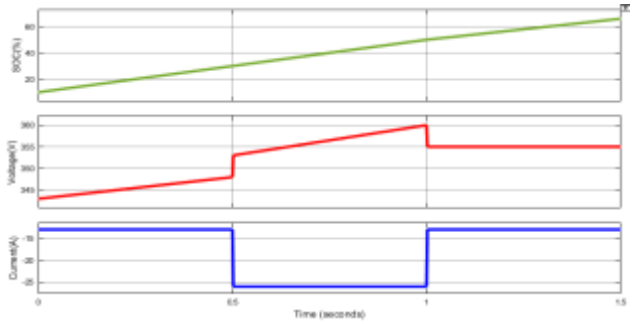

FIGURE 5.12 Battery parameter variation viz. SoC, voltage (V2) and current (I0) while charging at 1C-rate and 2C-rate.

By increasing it from 2.16◦ to 23◦ and then reducing it down to 2.16◦, the observed phase shift confirms the resilience of the developed PID controller and the theoretical phase-shift calculation. The electricity flows back to the grid from the vehicle when the phase shift between the main and secondary bridges is reversed.

To ensure bidirectional functionality, the battery was depleted at a rate of 1C while in CC mode. Fig. 5.12 shows the waveform of a battery with a voltage drop from 50% to 25% and a current in the dc connection that remains constant in amplitude. The safety, performance, and lifespan of the battery are ensured by preventing the SoC from dropping below 25% while discharging to the grid.

6. Conclusion

The research work in this paper proposes a topological modification of a Dual Active Bridge (DAB) converter for bidirectional power transfer in a DC micro grid connected fast EV charging station (EVCS). Unstable dynamics shorten battery life, especially in fast charging conditions. An active damping approach using a notch filter (NF) was introduced in cascade with DAB to attenuate these unstable dynamics and improve system stability. The proposed active damping method not only achieves resonance damping and loss reduction but also improves the proportional gain of the PID controller, thus satisfying the bandwidth requirement.

Bode analysis is performed to verify the developed system performance for parametric variations in the output LC filter. It is inferred that the proposed converter topology also aids in the improvement of the system's robustness by handling parameter uncertainties. The charge flow to the battery is controlled using the CCCV algorithm. C-rates were varied to test the effectiveness of the controller and the modified topology during battery charging. The results show that the proposed model can effectively control the charging and discharging of the EV battery. In addition, the Zero Voltage Switching (ZVS) technique is implemented to improve efficiency.

A Bode diagram with and without NF is plotted to validate the system performance. The efficiency of the designed DAB converter is observed to be 96.1% at the rated load condition. Dynamic response analysis for EV fast charging infers that the proposed system is essential for optimal performance in fast EVCS. The developed system can have significant practical implications like improved battery health and lifespan, particularly in industries reliant on battery technology. By enabling faster, more efficient, and reliable charging of batteries, the research outcome from this paper contributes to achieving a more sustainable energy future by improving the charging infrastructure and facilitating the integration of renewable energy into the grid.

References

[1] S. Kim and F.-S. Kang, ''Multifunctional onboard battery charger for plug-in electric vehicles,'' IEEE Trans. Ind. Electron., vol. 62, no. 6, pp. 3460–3472, Jun. 2015, doi: 10.1109/TIE.2014.2376878.

[2] N. Naik and C. Vyjayanthi, ''Optimization of vehicle-to-grid (V2G) services for development of smart electric grid: A review,'' in Proc. Int. Conf. Smart Gener. Comput., Commun. Netw., Pune, India, Oct. 2021, pp. 1–6, doi: 10.1109/SMARTGENCON51891.2021.9645903.

[3] R. V. S. E. Shravan and C. Vyjayanthi, ''Active power filtering using interlinking converter in droop controlled islanded hybrid AC–DC microgrid,'' Int. Trans. Electr. Energy Syst., vol. 30, no. 5, pp. 1–27, May 2020, doi: 10.1002/2050-7038.12333.

[4] S. Shao, L. Chen, Z. Shan, F. Gao, H. Chen, D. Sha, and T. Dragicevic, ''Modeling and advanced control of dual-active-bridge DC–DC converters: A review,'' IEEE Trans. Power Electron., vol. 37, no. 2, pp. 1524–1547, Feb. 2022, doi: 10.1109/TPEL.2021.3108157.

[5] M. Gopahanal Manjunath, V. Chintamani, and C. Modi, ''A real-time hybrid battery state of charge and state of health estimation technique in renewable energy integrated microgrid applications,'' Int. J. Emerg. Electr. Power Syst., vol. 18, pp. 1–10, May 2022, doi: 10.1515/ijeeps-2021-0434.

[6] L. Zheng, X. Han, Z. An, R. P. Kandula, K. Kandasamy, M. Saeedifard, and D. Divan, ''SiC-based 5-kV universal modular soft-switching solid-state transformer (M-S4T) for medium-voltage DC microgrids and distribution grids,'' IEEE Trans. Power Electron., vol. 36, no. 10, pp. 11326–11343, Oct. 2021, doi: 10.1109/TPEL.2021.3066908.

[7] Q. Xu, N. Vafamand, L. Chen, T. Dragicevic, L. Xie, and F. Blaabjerg, ''Review on advanced control technologies for bidirectional DC/DC converters in DC microgrids,'' IEEE J. Emerg. Sel. Topics Power Electron., vol. 9, no. 2, pp. 1205–1221, Apr. 2021, doi: 10.1109/JESTPE.2020.2978064.

[8] D. Mishra, B. Singh, and B. K. Panigrahi, ''Adaptive current control for a bidirectional interleaved EV charger with disturbance rejection,'' IEEE Trans. Ind. Appl., vol. 57, no. 4, pp. 4080–4090, Jul. 2021, doi: 10.1109/TIA.2021.3074612.

[9] N. Naik and C. Vyjayanthi, ''Research on electric vehicle charging system: Key technologies, communication techniques, control strategies and standards,'' in Proc. IEEE 2nd Int. Conf. Electr. Power Energy Syst. (ICEPES), Bhopal, India, Dec. 2021, pp. 1–6, doi: 10.1109/ICEPES52894.2021.9699496.

[10] S.-A. Amamra and J. Marco, ‘‘Vehicle-to-grid aggregator to support power grid and reduce electric vehicle charging cost,’’ IEEE Access, vol. 7, pp. 178528–178538, 2019, doi: 10.1109/ACCESS.2019.2958664.

[11] T.-T. Le, H. Jeong, and S. Choi, ‘‘A bidirectional three-phase push–pull converter with hybrid PPS-DAPWM switching method for high power and wide voltage range applications,’’ IEEE Trans. Ind. Electron., vol. 68, no. 2, pp. 1322–1331, Feb. 2021, doi: 10.1109/TIE.2020.2969113.

[12] J.-H. Choi, H.-M. Kwon, and J.-Y. Lee, ‘‘Design of a 3.3 kW/100 kHz EV charger based on flyback converter with active snubber,’’ IEEE Trans. Veh. Technol., vol. 71, no. 7, pp. 7161–7170, Jul. 2022, doi: 10.1109/TVT.2022.3168625.

[13] T. Jiang, J. Zhang, X. Wu, K. Sheng, and Y. Wang, ‘‘A bidirectional LLC resonant converter with automatic forward and backward mode transition,’’ IEEE Trans. Power Electron., vol. 30, no. 2, pp. 757–770, Feb. 2015, doi: 10.1109/TPEL.2014.2307329.

[14] B. Han, J.-S. Lai, and M. Kim, ‘‘Dynamic modeling and controller design of dual-mode Cuk inverter in grid-connected PV/TE applications,’’ IEEE Trans. Power Electron., vol. 33, no. 10, pp. 8887–8904, Oct. 2018, doi: 10.1109/TPEL.2017.2779843.

[15] H. Wen, J. Li, H. Shi, Y. Hu, and Y. Yang, ‘‘Fault diagnosis and tolerant control of dual-active-bridge converter with triple-phase shift control for bidirectional EV charging systems,’’ IEEE Trans. Transport. Electrific., vol. 7, no. 1, pp. 287–303, Mar. 2021, doi: 10.1109/TTE.2020.3045673.

[16] Y.-C. Jeung and D.-C. Lee, ‘‘Voltage and current regulations of bidirectional isolated dual-active-bridge DC–DC converters based on a doubleintegral sliding mode control,’’ IEEE Trans. Power Electron., vol. 34, no. 7, pp. 6937–6946, Jul. 2019, doi: 10.1109/TPEL.2018.2873834.

[17] Y. Nazih, M. G. Abdel-Moneim, A. A. Aboushady, A. S. Abdel-Khalik, and M. S. Hamad, ‘‘A ring-connected dual active bridge based DC–DC multiport converter for EV fast-charging stations,’’ IEEE Access, vol. 10, pp. 52052–52066, 2022, doi: 10.1109/ACCESS.2022.3173616.

[18] B. Zhao, Q. Song, J. Li, Y. Wang, and W. Liu, ‘‘Modular multilevel high-frequency-link DC transformer based on dual active phase-shift principle for medium-voltage DC power distribution application,’’ IEEE Trans. Power Electron., vol. 32, no. 3, pp. 1779–1791, Mar. 2017, doi: 10.1109/TPEL.2016.2558660.